CO5-1 INAA and Ar-Ar Dating for Small Extraterrestrial Materials

R. Okazaki and S. Sekimoto[1]

Department of Earth and Planetary Sciences, Kyushu University
[1]Research Reactor Institute, Kyoto University

INTRODUCTION: In order to elucidate the origin and evolution of planetary materials, it is important to determine the chemical composition and age of specific minerals and microscopic portions, such as impact melt pockets, CAIs (Ca- and Al-rich Inclusion), and chondrules. The major chemical composition of microscopic regions or dust particles can be analyzed with generally-used analytical instruments (e.g., EMPA, electron microprobe analyzer), whereas it is difficult to measure abundances of trace elements and isotopic compositions. Combination of EMPA, INAA, and noble gas analysis are one of the best way to determine chemical and isotopic compositions of as many elements as possible. For example, mineral chemistry such as Fe content in olivine and pyroxene can be determined by EMPA at first by using a one-side-polished section, which will be followed by INAA for trace element (e.g., Pt) analysis, and finally Ar isotopes will be determined to date Ar-Ar age of the sample. This analytical method is useful for limited samples without any substitution, such as anomalous meteorite material, extraterrestrial dust particles (micrometeorites) and spacecraft-returned samples.

As a first step, we have selected the standard samples with similar size and weight to extraterrestrial microgram samples for INAA and Ar-Ar dating. Next, we have established a sample container and a handling method to minimize loss and contamination of the samples. These works have been conducted through our research projects at KURRI.

EXPERIMENTS: In this work, neutron irradiation was applied to several tens to several hundred micron-sized (0.1 to 10 microgram) rock fragments recovered from meteorites (Allende CV3 chondrite, Holbrook L6 chondrite, and Agoult and HAH262 eucrties), terrestrial rocks and minerals (JB-1, orthoclase, and wollastonite), Pt-Ir alloy, and an NIST glass standard (SRM610). Each of the sample particles was placed in a conical dimple (φ1, depth ~ 0.5 mm) of a sapphire disk (φ5.5, 1.5 mm thick), and covered with a sapphire disk (φ5.5, 0.3 mm thick). Each of the sapphire container was wrapped with pure aluminum foil. These Al-wrapped containers were stacked and sealed in the Hydro capsules to perform neutron irradiation. After irradiation, the samples were moved to non-irradiated glass container with similar dimension from the sapphire one in order to reduce the radioactivity from the sapphire containers and Al foil.

Gamma ray measurements for short halflife nuclides were performed promptly after collection of the samples. Allende and JB-1 were used as reference standard of the INAA. Noble gas isotopes in orthoclase samples were measured by using a mass spectrometer at Kyushu university. These INAA and noble-gas analyses were conducted as a project adopted in 2014 (No. 25066, PI: S. S.). In this project in 2017 (No. 29008, PI: R. O.), only neutron irradiation has been carried out in 2018 Jan. Noble gas analysis will be done in this summer.

RESULTS: Fig. 1 shows the Co and Ni concentrations in some fragments collected from Holbrook L6 chondrite. The Hol-2G and -3C plot on the tie line defined by iron meteorites, chondrite components, and bulk chondrite data (Fig. 1). Electron microscope observation revealed that these two samples contain Fe-Ni metal and/or trolite (FeS). In contrast, Hol-13G contains neither metal or troilite, and its Ni content was below than the detection limit of INAA.

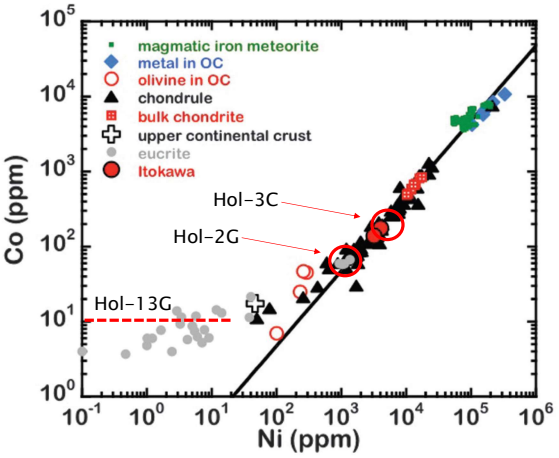

Fig. 1. Co and Ni concentrations in Holbrook and other extraterrestrial samples ([1].

The concentration of Ir was determined to be 4.44±0.38 wt% (n=5) by using ~5 μg of in Pr-Ir alloy samples, which is in good agreement with the reference value of 5 wt%.

Minor and trace element concentrations in SRM610 were around 300-400 ppm with relatively small deviations, but are lower than reference values of ~500 ppm [2]. Exceptionally, Ni and Zn concentrations were ~1000-1400 ppm, which is due to interference from other elements (possibly Eu) contained in SRM610. Hence, SRM610 is not suited for INAA.

REFERENCES:

[1] M. Ebihara *et al.*, Science, **333** (2011) 1119-1121.
[2] A. B. E. Rocholl *et al.*, Geostandards Newsletter, **21** (1997) 101-114.

CO5-2 Volcanic and Tectonic History of Intra-oceanic Island Arc Revealed by $^{40}Ar/^{39}Ar$ Dating Technique

O. Ishizuka, S. Sekimoto[1], R. Okumura[1], H. Yoshinaga[1], T. Fujii[2]

Geological Survey of Japan, AIST
[1]Institute for Integrated Radiation and Nuclear Science, Kyoto University
[2]Graduate School of Engineering, Osaka University

INTRODUCTION: Submarine volcanic rocks are known to give K-Ar ages different from their true eruption ages in some cases. This is due to the existence of excess ^{40}Ar in the rapidly quenched glass or Ar loss and K remobilization caused by reaction with seawater or hydrothermal fluids. Capability of evaluating these effects makes stepwise-heating analysis in $^{40}Ar/^{39}Ar$ dating particularly useful for dating submarine volcanics.

We conducted a research cruise KS-17-15 in November, 2017 to achieve robust tectonic reconstruction of the evolving Philippine Sea Plate for the period immediately before and after subduction initiation at ~52 Ma to form the Izu-Bonin-Mariana arc, which is one of the "typical" intra-oceanic island arc. This cruise successfully recovered igneous rocks from the Kita-Daito Basin, which is one of the major oceanic basins in the oldest part of the Philippine Sea Plate. Here we report the first preliminary $^{40}Ar/^{39}Ar$ age obtained from the igneous rock recovered during this cruise.

EXPERIMENTS: Samples were wrapped in an aluminum foil packet and the packets were piled up in a pure aluminum (99.5% Al) irradiation capsule (9 mm diameter and 30 mm long). The irradiation capsule was partitioned into 3 compartments to minimize the uncertainty of the sample positions at irradiation. The irradiation capsule was wrapped with 0.5 mm-thick Cd-foil before irradiation. The capsule was irradiated for 2 hours at 5MW in Hyd facility of KUR on January 18, 2018. Analyses were conducted using $^{40}Ar/^{39}Ar$ geochronology facility at the Geological Survey of Japan/AIST following the analytical procedure described in [1].

For the experiments described here, 5 mg of sample was analysed. Due to alteration of poorly-crystallized part of groundmass, the sample was treated at 100°C on hot plate with stirrer in 6N HCl for 30 minutes and then 6N HNO_3 for 30 minutes to remove possible alteration products (clays and carbonates) prior to irradiation. This procedure effectively separated and concentrated fresh plagioclase in groundmass and of microphenocryst. After this acid treatment, the separates were examined under binocular microscope before packed for irradiation.

RESULTS: One basaltic sample recovered from the western part of the Kita-Daito Basin was dated. The Kita-Daito Basin, separating the Amami Plateau and the Daito Ridge, has a thin crust of 4 to 6 km based on seismic structure, and was inferred to be a backarc ocean crust [2]. No age data have been obtained from this basin to constrain its age of formation.

The analysed sample was recovered by dredging operation. This dredge was conducted on the steep NE-facing slope of a 1000m-high irregular-shaped bathymetric high in the westernmost part of the Kita-Daito Basin (Fig. 1). The dredge arrived at bottom at a water depth of 5399 m. Total 5 kg of samples were recovered. Major rock types are polymictic breccia and cpx-ol basalt lava clasts. These breccia samples are mainly composed of cpx-ol basalt, px basalt and pl-phyric basalt. The dated sample (D1R3) is cpx-phyric basalt with groundmass containing abundant plagioclase.

Stepwise heating procedure of $^{40}Ar/^{39}Ar$ dating was applied for this sample. Fig. 2 shows age spectrum for this analysis. This sample gave a plateau age of 41.00 ± 0.09 Ma comprising of 69.1% of released gas. This age plateau consists of 19 steps out of 31 steps. The plateau age shown here is still temporary age because flux monitor measurement has not been completed yet. However, the data strong implies that formation of the Kita-Daito Basin is younger than the neighboring Amami Plateau and Daito Ridge, and also postdate the subduction initiation of the Izu-Bonin-Mariana arc. This new result is crucial for tectonic reconstruction of the Philippine Sea area.

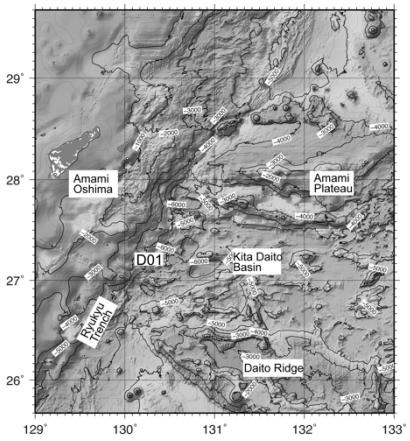

Fig. 1 Locality of the dated sample.

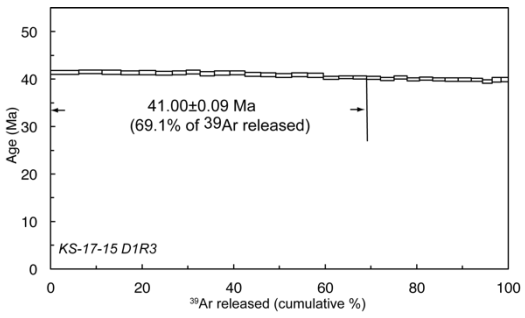

Fig. 2 Age spectrum for the basalts from the Kita-Daito Basin.

REFERENCES:

[1] O. Ishizuka *et al.*, Earth Planet. Sci. Lett., **481** (2018), 80-90.
[2]A. Nishizawa *et al.*, Earth Planets Space, **66**:25 (2014).

CO5-3 I-Xe Age of a Brecciated Meteorite, NWA2139

H. Sumino, K. Shimodate, K. Sudo, S. Kishi, M. Koike, T. Kagoshima, T. Yamaguchi, R. Okumura[1] and S. Sekimoto[1]

University of Tokyo
[1] Institute for Integrated Radiation and Nuclear Science, Kyoto University

INTRODUCTION: An extinct nuclide ^{129}I ($T_{1/2}$ = 15.7 million years) is known to have lived in the early stage of solar system formation. As ratio of ^{129}I to stable isotope ^{127}I in the solar system decreased with time, formation ages of individual meteorites can be estimated if we determine $^{129}I/^{127}I$ ratios for the meteorites. Because all ^{129}I trapped in a meteorite now has completely decayed to stable isotope ^{129}Xe, present $^{129}Xe^*/^{127}I$ ratio, where $^{129}Xe^*$ is excess of ^{129}Xe over primordial Xe component such as Q-Xe [1], is equivalent to $^{129}I/^{127}I$ ratio at the meteorite formation. In the I-Xe dating method, meteorites and an age standard meteorite are irradiated with neutrons in a nuclear reactor to convert ^{127}I to $^{128}Xe^*$, and then $^{129}Xe^*/^{128}Xe^*$ ratios are measured for the meteorites [2]. Time span of formation age "Δt" after formation of the standard meteorite is expressed as;

$$\Delta t = (1/\lambda)\times \ln [(^{129}Xe^*/^{128}Xe^*)_{std}/(^{129}Xe^*/^{128}Xe^*)_{sample}].$$

Brecciated meteorites record impact events occurred on their parent planetesimals, where meteoroids bombarded surface materials producing rock fragments and soils which finally solidified to rocks with brecciated structure. The impact fragmentation would have continued before and after dissipation of dense solar nebular in the early solar system. Some brecciated meteorites are known to have very high concentrations of solar He and Ne, but other brecciated ones do not contain. The solar noble gases are derived from solar wind which was implanted within 1 μm of regolith particles on the surface of the parent bodies of the meteorites. We measured noble gas compositions and I-Xe ages for several brecciated meteorites and found out that meteorites showing old I-Xe ages are solar gas free, but those with younger ages are enriched in solar gases. This may constrain timing of dissipation of solar nebula, which could be determined experimentally by I-Xe dating and noble gas analysis for brecciated meteorites [3]. Here we report a new I-Xe data of the NWA2139 meteorite, which is classified as LL6 chondrite with brecciated texture.

EXPERIMENTS: The light-colored and dark-colored fragments of the NWA2139 meteorite and age standard meteorite, Shallowater, weighing ca. 20 mg each were irradiated with neutrons in the long-term irradiation plug of KUR reactor. After cooling down for several months noble gas isotopes in the samples were analyzed using a modified-VG3600 mass spectrometry system at the Graduate School of Arts and Sciences, the University of Tokyo [4]. Non-irradiated meteorites were also measured for noble gases with a modified-VG5400 noble gas mass spectrometer at the University of Tokyo.

RESULTS: Isotopic ratios $^{129}Xe/^{132}Xe$ plot against $^{128}Xe/^{132}Xe$ in Fig. 1 for both NWA2139 and Shallowater meteorites. The data points for Shallowater with 4563.3 ± 0.4 Ma (Ma = million years ago) absolute age [5] plot on a straight line, showing perfect closure to I-Xe system. Contrary to the Shallowater data points, those for the dark-colored fragment of NWA2139 do not show a linear trend and plot around the trapped Q-Xe [1]. This would result from almost complete resetting of I-Xe system caused by a heavy shock event occurred after the extinction of ^{129}I. This is consistent with that the sample does not show a presence of solar noble gases. The light-colored fragment of NWA2139 yielded I-Xe age of 4512 ± 12 Ma. Although this age postdates the dissipation of solar nebula inferred from a relationship between I-Xe ages and solar noble gas concentrations for other brecciated meteorites [3], the NWA2139 light-colored fragment does not contain detectable amounts of solar noble gases. This can be explained by (1) the sample was not exposed to the solar wind on the surface of its parent body, or (2) solar noble gases were degassed by a shock event, which could be milder than that the dark-colored fragment experienced as the I-Xe system of the light-colored fragment has not been completely reset.

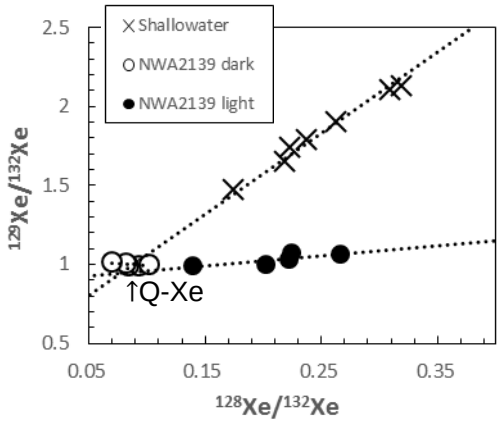

Fig. 1. Plot of $^{129}Xe/^{130}Xe$ vs. $^{128}Xe/^{130}Xe$ for NWA2139 and Shallowater meteorites.

REFERENCES:

[1] H. Busemann *et al.*, Meteorit. Planet. Sci., **35** (2000) 949–973.
[2] P.M. Jeffrey and J.H. Reynolds, J. Geophys. Res., **66** (1961) 3582–3583.
[3] K. Bajo, Ph.D. Thesis, Univ. Tokyo (2010).
[4] N. Ebisawa *et al.*, J. Mass Spectrom. Soc. Jpn., **52** (2004) 219–229.
[5] J.D. Gilmour *et al.*, Meteorit. Planet. Sci., **41** (2006) 19–31.

CO5-4 Clear Descent of Antimony(Sb) Concentration in Atmospheric Aerosol Observed at Sakai, Osaka from 1995 to 2017

N. ito, A. Mizohata, R. Okumura[1] and Y. Iinuma[1]

Radiation Reserch Center, Osaka Prefecture University,
[1]Research Reactor Institute, Kyoto University

Antimony(Sb) is a poison element and can be found in the aerosols collected on the urban area as a trace element in the coarse particle(might be affected from brake pads) and fine particle (might be affected from burning of plastics). To study a characteristic of Sb on the aerosols in the urban area, we have observed the size distribution of Sb in the aerosols at Sakai since 1995. Here we report the yearly change in concentration from which result reveal the clear descent in Sb concentration.

We have collected the aerosol by Andersen Sampler, collecting the aerosols on 9 particle size rages (>11, 7.0-11.0, 4.7-7.0, 3.3-4.7, 2.1-3.3, 1.1-2.1, 0.65-1.1, 0.43-0.65, <0.43μm) with one week sampling period . The aerosols were collected on the polyethylene sheet for each sampling stages except for the final stage that uses Teflon filter to filter the smallest particles. The concentration of Sb were measured by neutron activation analysis using Kyoto University Reactor, measuring gamma ray (1691 keV) from ^{124}Sb activated in PN2 line with 2 hour irradiation of thermal neutron.

Results of size distribution(Fig.1) observed in 1995 Apr.24-May08 and 2017 Mar.28-Apr04 show that Sb occurs in coarse and fine particles on the affect of particles from soils and brake pad for coarse particles and from plastic burning for fine particles. Result of two size distribution(1995Apr and 2017 Mar) of Sb for 22 years interval reveal the clear descent in concentration.

Result of Sb concentration change(coarse :d >2.1μm, fine: d<2.1μm)in year of1995,1996,1997, 1998,1999,2000, 2012, 2017 are drawn on the Fig.2. From 1998 concentrations of Sb in coarse and fine particles have descended clearly on the decrease with 2ng/m^3 in 1995 -1997 to 0.5ng/m^3 in 2017 for coarse particles, 6 ng/m^3 in 1995-1997 to 1 ng/m^3 in 2017 for fine particles. We suggest that reduction of exhausted matter from incinerator that were controlled by government direction caused the clear descent of Sb concentration in recent 20 years.

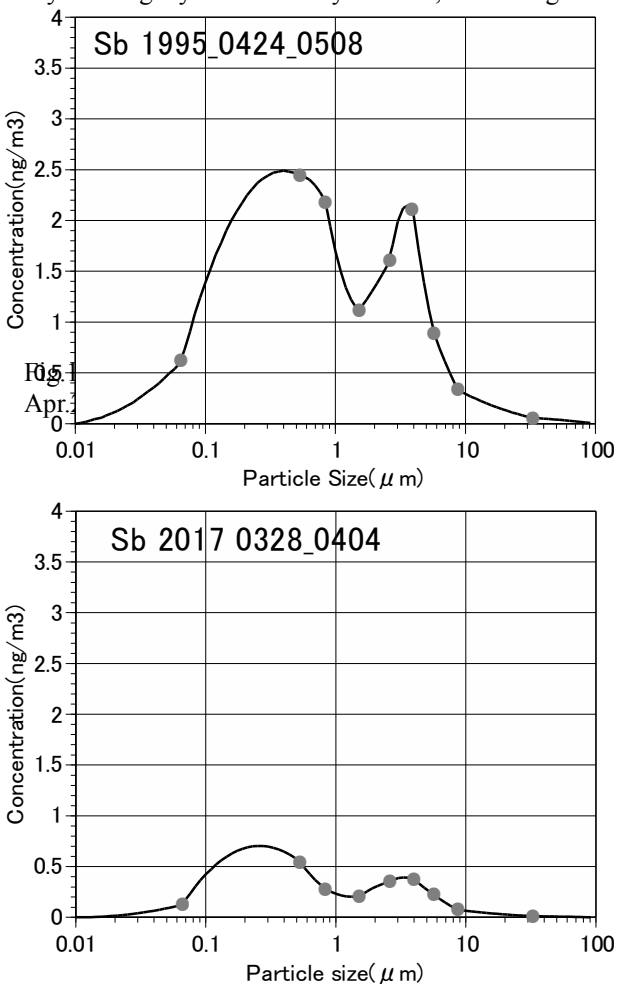

Fig.1 Size distribution of Sb observed in 1995 Apr.24-May08 and 2017Mar28-Apr04 at Sakai

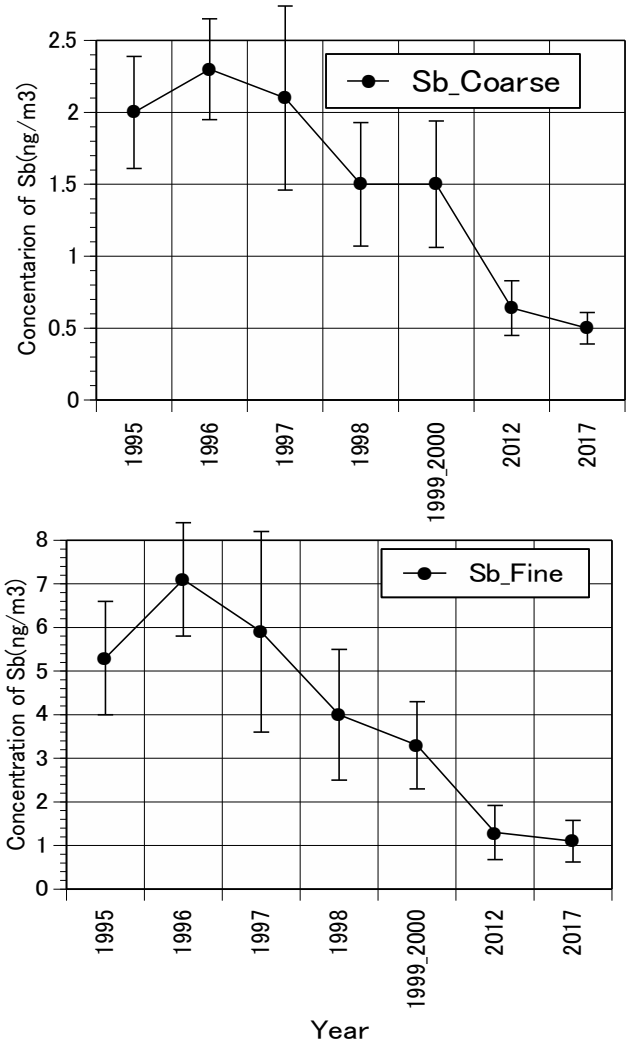

Fig.2 Change of Sb in 1995, 1996,1997,1998, 1999,2000, 2012 and 2017 in coarse and fine particles at Sakai.

CO5-5 A Study on the Sedimentary Environment of Tokyo-Bay Sediments under Hypoxia Using Instrumental Neutron Activation Analysis

M. Matsuo[1], K. Shozugawa[1], Y. Mihara[1], M. Komori[1, 2], R. Okumura[3], Y. Iinuma[3] and K. Takamiya[3]

[1]*Graduate School of Arts and Sciences, The University of Tokyo*
[2]*Environmental Research Institute of Yokohama*
[3]*Research Reactor Institute, Kyoto University*

INTRODUCTION: Hypoxia is water mass with little dissolved oxygen (DO) [1]. It has been a big problem particularly in inner bay such as Tokyo Bay. To understand and solve the problem, it is important to know when or where hypoxia occurred. However, the data of water quality in Tokyo Bay are absolutely lacking. Therefore, we attempted to estimate the redox environment of Tokyo-bay sediments under hypoxia, assuming that the effect of past hypoxia could be preserved as a difference in concentrations and/or chemical states of elements in the sediments.

To estimate the sedimentary environment related to redox conditions, various elements have been used. For example, Fe and Mn are used because their various chemical states on Eh-pH diagrams have become clear [2]. And U is used for the evaluation of weak reductive conditions because the redox potential of U(VI)/U(IV) is between Mn(IV)/Mn(II) and S(VI)/S(-II) [3]. In this study, sediment cores were collected from Tokyo Bay and concentrations of Fe, Mn, U, Th, and Ce in sediments were analyzed by instrumental neutron activation analysis (INAA).

EXPERIMENTS: We collected sediment cores off the coast of Yokohama (flat seafloor) and Makuhari (flat seafloor and dredged trench) in Tokyo Bay. All cores were cut in the vertical direction at 2 cm intervals in the laboratory. Then, the samples were desalted by centrifugation with pure water washing three times and dried at 105 ℃.

Approximately 30 mg of sediments were packed in double polyethylene film bags to perform INAA. All samples were irradiated with neutrons at the pneumatic tube, Kyoto University Research Reactor. Three types of gamma-ray measurement were carried out corresponding to half-lives of elements. For analysis of Mn, samples were irradiated for 10 seconds at 1 MW, and then gamma-ray was measured for 600 seconds by Ge detector after 600 seconds cooling. Regarding U, samples were irradiated for 20 minutes at 1 MW or 4 minutes at 5 MW, and then gamma-ray was measured for 1200 seconds after 3-5 days cooling. Regarding Fe, Th and Ce, samples were irradiated for 20 minutes at 1 MW or 4 minutes at 5 MW, and the measuring time of gamma-ray was for 10800 seconds after 2-4 weeks cooling.

RESULTS: Analysis of redox sensitive elements in the sediments was done by INAA method. As a result, the concentration of Mn was low in the dredged trench off Makuhari, whereas there was no significant difference in Fe. It is well-known that the concentrations of both Fe and Mn in sediments increase when condition of seawater is oxidative. However, we note that Mn precipitates under more oxidative conditions. Therefore, it is estimated that the oxidation-reduction potential in the dredged trench remained to the extent that Fe precipitation occurred but no Mn precipitation occurred.

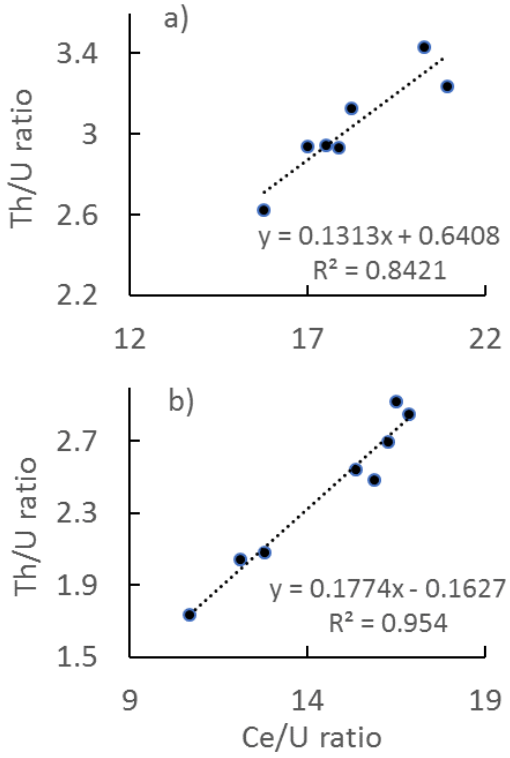

Fig. 1. Th/U-Ce/U plots in the sediments collected from (a) flat seafloor off Yokohama and (b) dredged trench off Makuhari.

In addition, we plotted the relations between Th/U and Ce/U ratios, and they are shown in Figure 1. The values of Th/U and Ce/U ratios at each site existed in different places on a same line. This fact indicates that the sediments cannot be the mixture of two or more sources which have different Th/U and Ce/U ratios. Therefore, it is thought that the fact is caused by redox conditions. As a result, it was found that the magnitude of the reductive environment increased in the order of flat seafloor off Yokohama < flat seafloor off Makuhari < dreaded trench off Makuhari. This trend was in good agreement with water quality data and estimation results from chemical states of iron measured by ^{57}Fe Mossbauer spectroscopy.

REFERENCES:

[1] R.J. Diaz *et al*., Science, **321** (2008), 926-929.
[2] D.G. Brookins, in *Eh-pH diagrams for geochemistry* (Springer-Verlag, 1988).
[3] D.R. Turner, M. Whitfield and A.G. Dickson, Geochim. Cosmochim. Acta, **45** (1981), 855-881.

CO5-6 Ionic Exchange of Tritium in Water and Hydrogen in Hydroxides

H. Hashizume, A. Uehara[1], S. Fukutani[2], K. Fujii and T. Ando

National Institute for Materials Science
[1]National Institute of Radiological Science
[2]Institute for Integrated Radiation and Nuclear Science, Kyoto University

INTRODUCTION: Tritium is one of radioactive elements. Its half-time is about 12 years. Since the amount of yield of tritium which is formed in a nuclear reactor is a very little, generally, tritium does not affect the environment. However, in the serious trouble of the Fukushima 1 Nuclear Power Station, a huge amount of tritium was formed and tritium had been included in water. Since water including tritium is almost the same characteristics as water without tritium, it is almost impossible to remove tritium from water. For that reason, the water contaminated by tritium has been accumulated. We have to find out new methods to remove tritium from water, eargently. Koyanaka and Miyatake (2015) found out that about 30% amounts of tritium in water including tritium was caught by manganese oxide for about 20 min [1]. Hashizume et al. (2016) investigated that tritium was discriminated in the formation of a hydroxide from an oxide in water including tritium. When the reaction of magnesia with water including tritium resulted in magnesium hydroxide, a small amount of tritium as a hydroxyl group was caught in the formation of magnesium hydroxide [2]. About 2% of tritium was removed from water including tritium. Since the decomposition temperature of magnesium hydroxide is more than 300 ºC, tritium would be captured in magnesium hydroxide and would not remove from magnesium hydroxide at around room temperature.

As anther possible removal of tritium, we investigate the ionic exchange of tritium in water and hydrogen in a hydroxide and the change of amount of ionic exchange of tritium to the contact time with hydroxide and water with tritium.

EXPERIMENTS: The hydroxides used were magnesium, calcium and aluminum hydroxide ($Mg(OH)_2$, $Ca(OH)_2$ and $Al(OH)_3$). We used water including tritium, which is prepared in Institute for Integrated Radiation and Nuclear Science, Kyoto University. The hydroxide, which weighed 2 g, and 10 cm^3 of water including tritium were put in the glass bottle with stopper. For the investigation of the ionic exchange, the shaking time was changed from 1 to 18 hours. After shaking, supernatant was separated from suspension by filtering. The supernatant and the initial solution were diluted by the liquid scintillator, that is 20 cm^3 of the liquid scintillator was added in 1 cm^3 of supernatant or initial solution. The mixed solution was measured by a scintillation detector (Packard, Liquid Scintillation Analyzer). We estimated the removal of tritium (R %).

$$R=100\cdot(C-C_0)/C_0\cdot W$$

where C, C_0 and W are concentration of supernatant and initial solution (Bq) and weight (g), respectively.

RESULTS: The removal of tritium to the shaking time is shown in Fig. 1. The removal by $Mg(OH)_2$ and $Ca(OH)_2$ rises as the increase of shaking time. The removals by $Mg(OH)_2$ and $Ca(OH)_2$ are finally almost constant. In the case of $Mg(OH)_2$, The removal is increasing until 5 h of the shaking time. After 5 h, the removal is almost constant, that is about 1.0 %. In the case of $Ca(OH)_2$, the removal reaches the plateau within about 3 h of the shaking time. The removal of the plateau is about 0.6 %. On the other hand, in the use of $Al(OH)_3$, tritium hardly exchanged with hydrogen in $Al(OH)_3$. Although we do not know the reasons why hydrogen in $Al(OH)_3$ is not exchanged with tritium, the crystal structure of $Al(OH)_3$ is different from that of $Mg(OH)_2$ or $Ca(OH)_2$. $Mg(OH)_2$ belongs to a trigonal system and it has a three-fold rotation axis. $Ca(OH)_2$ belongs to a hexagonal system and it has a six-fold rotation axis. The trigonal system is very similar to the hexagonal one. However, the crystal system of $Al(OH)_3$ is monoclinic. The crystal system of $Al(OH)_3$ is different from that of $Mg(OH)_2$ or $Ca(OH)_2$, though those three hydroxides show the sheet structure. The similarity of crystal systems of $Mg(OH)_2$, $Ca(OH)_2$ and $Al(OH)_3$ might cause the different removals of tritium of three ionic exchange materials.

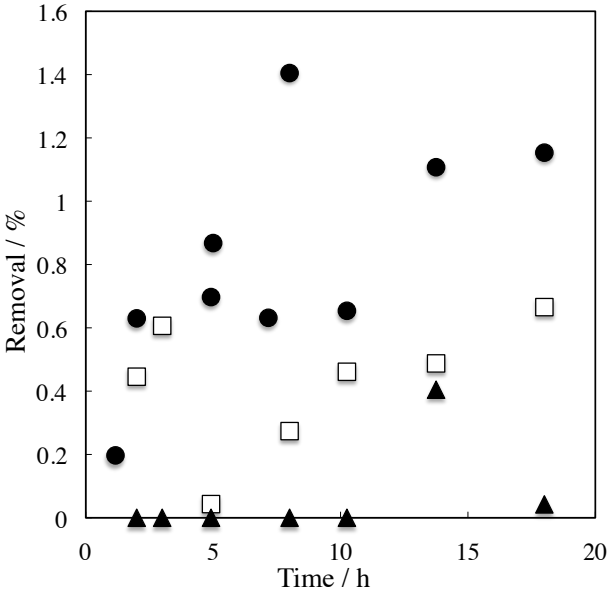

Fig.1 removal of tritium from water depending on shaking time by the ionic exchange to use magenisum hydroxide (●), calcium hydroxide (□), aluminum hydroxide (▲).

REFERENCES:

[1] H.Koyanaka & H. Miyatake, *Separation Science Technology*, **50** (2015) 2142-2145.
[2] H.Hashizume *et al.* Tokugann 2016-135839 (2016) (Japanese patent in Japanese).

CO5-7 Determination of Abundance of Rare Metal Elements in Seafloor Hydrothermal Ore Deposits by INAA Techniques-4: Evaluation of Analytical Accuracy

J. Ishibashi, Y. Tada[1], S. Kawaguchi[1], K. Yonezu[2], R. Okumura[3], H. Yoshinaga[3] and K. Takamiya[3]

Department of Earth and Planetary Sciences, Faculty of Science, Kyushu University
[1]Department of Earth Resources Engineering, Faculty of Engineering, Kyushu University
[3]Research Reactor Institute, Kyoto University

INTRODUCTION: To meet recent increased demand for rare metal elements as mineral resources, high sensitive multi-element analysis becomes more important as geochemical tools for mineral exploration. Instrumental neutron activation analysis (INAA) has the advantage of non-destructive analysis, which eliminates possible failings to exclude concentrate of elements included in specific mineral poorly soluble during acid digestion. We have conducted preliminary studies using mineralized samples collected from active seafloor hydrothermal fields, with a view to confirm and extend the range of application of this technique. Here, we report evaluation for analytical accuracy of INAA techniques, using reference ore materials.

EXPERIMENTS: We conducted a series of analysis of "Certified Reference Materials" which are provided by Natural Resource Canada. Samples were irradiated at Pn-3 (thermal neutron flux = 4.8×10^{12} n/cm^2/sec at 1 MW) for 3 minutes. The gamma ray activity was measured twice; 2 minutes measurement after 4-20 minutes cooling, and 10 minutes measurement after about 4 hours cooling. Content of each nuclide was calculated by comparison of gamma ray intensities between samples and artificial standard materials which contain known amount of Mn.

RESULTS: Analytical results of the Certified Reference Materials, CCU-1d, WMA-1a, CH-4, and DS-4 are listed in Table 1. Nuclides used for the determination of elemental content are listed with their energies and half-life in minutes. We conducted at least two runs to check the accuracy. Content of elements is shown together with one sigma deviations for counting the peak intensity of the gamma ray spectra. The determined contents are basically agreed with the literature values (which are reported as informational values, provisional values, or certified values in the document provided by Natural Resource Canada).

Table 1 Analytical results of "Certified Reference Materials" provided by Natural Resources Canada. Results of two runs (the cooling time is denoted in parentheses) are listed to check the accuracy. Content of elements is shown with one sigma deviation for counting the peak intensity. Digits expressed in blankets are certified values reported for the Reference Materials.

Element (unit)	Al (wt%)	V (ppm)	Cu (ppm)	In (ppm)	Mn (ppm)
Nuclide	Al-28	V-52	Cu-66	In-116m	Mn-56
energy (kev)	1779	1434	1039	1097	846
half-life (min.)	2.24	3.75	5.10	54.1	154
CCU-1d	[0.19]	[no data]	[239000]	[7.0]	[99.4]
Run-1 (1331s)	-	-	70400±600	23.9±0.8	87.8±3.0
Run-2 (11172s)	-	-	-	19.8±1.0	92.7±1.4
WMS-1a	[1.35]	[140]	[13400]	[0.2]	[600]
Run-1 (235s)	1.00±0.05	90.4±1.4	3410±43	-	511±5
Run-2 (796s)	1.10±0.02	90.4±1.4	3640±66	-	568±5
CH-4	[7.73]	[87]	[2000]	[no data]	[430]
Run-1 (758s)	8.06±0.05	92.9±4.1	650±53	-	398±6
Run-2 (13203s)	-	-	-	-	410±4
DS-1	[4.48]	[147]	[27.1]	[no data]	[437]
Run-1 (568s)	4.45±0.03	146±3	-	-	420±6
Run-2 (705s)	4.67±0.04	151±4	-	-	443±6

Bar marks indicate too small peak intensity of the gamma ray spectrum.

CO5-8 Ar-Ar Determinations of Petit-spot Submarine Volcanoes

N. Hirano, H. Sumino[1] and S. Sekimoto[2]

Center for Northeast Asian Studies, Tohoku University
[1] Graduate School of Arts and Sciences, University of Tokyo
[2] Research Reactor Institute, Kyoto University

INTRODUCTION: Petit-spot volcanoes, erupted on NW Pacific plate, provide direct information on the asthenosphere and the lithospheric deformations below the NW Pacific because their magma originates from the asthenosphere and ascends along the concavely flexed zone prior to the outer-rise along the trench [1][2]. Similar volcanoes have been reported at subduction zones worldwide (e.g., the Japan, Tonga, Chile, and Java trenches) [1][2][3][4][5].

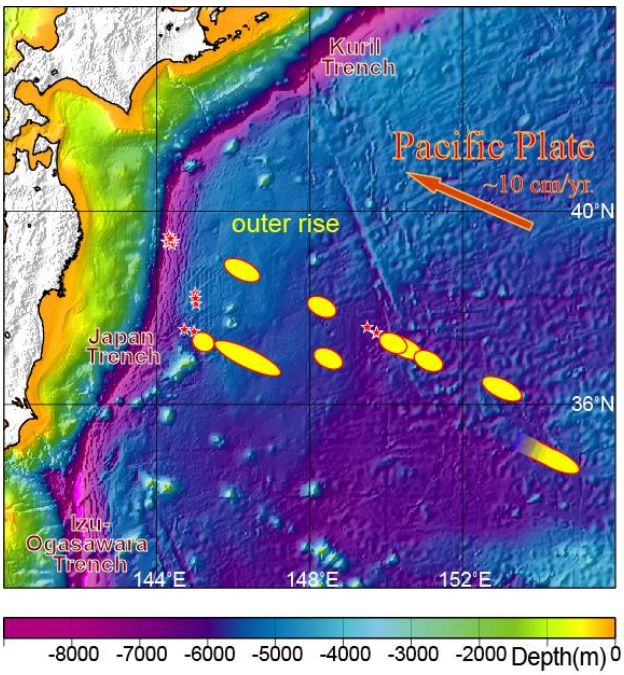

Fig. 1. Bathymetric map of offshore NE Japan [9]. Recognized sites of petit-spot volcano are known as red stars. Yellow ellipses show eruptive portions estimated by previously reported Ar-Ar ages of lavas [1][2] and constant plate motion of the present day (thick brown arrow) (10.29 cm/yr [10]).

Recent researches into the geochemistry and petrography of petit-spot lavas indicate that the conventional subducting lithospheric theories require some revision in terms of the nature of subducting lithospheric and asthenospheric materials (e.g., heterogeneous asthenosphere and the presence of a higher geothermal gradient than the conventional model) [6][7][8]. Most of lava samples do not contain phenocrysts in spite of their differentiated compositions, implying the fractionations in the magma chamber in lithosphere where the high levels of CO_2 contents of lavas must occur the lithospheric contamination by carbon-rich melt during magma ascent [8][11]. More recently, Sato et al. reported the primitive (low Si and high CO_2) composition for two example of volcanoes which erupt atop of outer rise (Fig. 1) and unusually include olivine phenocrysts [12]. As tectonic stress field atop outer rise is quite different from that of lithosphere below previously reported petit-spots (more than 20 volcanoes), lithospheric deformation must control their geochemical compositions and carbon emissions. We, therefore, conduct to determine the eruption ages of volcano using Ar-Ar dating to understand their eruptive site and tectonic reconstructions.

EXPERIMENTS: Radiometric Ar-Ar dating is commonly used to determine the ages of submarine lavas, because the traditional K-Ar dating is impossible to remove the alteration part of rocks [13]. After the rock-samples, crushed to 100-500 μm grains, they were irradiated by neutrons in a reactor to produce ^{39}Ar from ^{39}K during a few hours. During the irradiation, samples were packed with EB-1 biotite flux monitors [14], K_2SO_4 and CaF_2 as correcting factors in an aluminum capsule. Then, radiogenic ^{40}Ar, daughter nuclide of radioactive ^{40}K and parent, ^{39}Ar instead of ^{40}K, were simultaneously analyzed using a mass-spectrometer with an extraction technique of multi-step heating of approximately every 50 to 100 °C between 500 to 1500 °C.

RESULTS: The irradiations of sample in KUR were done in January, 2018. We are going to analyze the irradiated samples after cooling, awaiting future determinations.

REFERENCES:

[1] N. Hirano *et al.*, Science, **313** (2006), 1426-1428.
[2] N. Hirano *et al.*, Basin Res., **20** (2008), 543-553.
[3] N. Hirano *et al.*, Geochem. J., **47** (2013), 249-257.
[4] R. Taneja *et al.*, Gondwana Res., **28** (2014), 391–406.
[5] N. Hirano *et al.*, Marine Geol., **373** (2016), 39–48.
[6] J. Yamamoto *et al.*, Geology **42** (2014), 967-980.
[7] S. Pilet *et al.*, Nature Geosci. **9** (2016), 898-903.
[8] S. Machida *et al.*, Nature Comm. **8** (2017), 14302.
[9] D. T. Sandwell, and W. H. F. Smith, J. Geophys. Res., **102** (1997), 10039-10050.
[10] A. E. Gripp, and R. G. Gordon, Geophys. Res. Lett., **17** (1990), 1109-1112.
[11] S. Okumura, and N. Hirano, Geology, **41** (2013), 1167-1170.
[12] Y. Sato *et al.*, Int'l. Geol. Rev. (2017), in press.
[13] I. McDougall and T. M. Harrison, in *Geochronology and Thermochronology by the $^{40}Ar/^{39}Ar$ Method*, (Oxford, New York, 1988).
[14] N. Iwata, Ph.D. Thesis, Tokyo Univ. (1998).

CO5-9 Basic Study on Radiation-induced Luminescence from Natural Mineral

H. Fujita, M. Nagaoka, T. Saito[1]

Nuclear Fuel Cycle Engineering Laboratories, JAEA
[1]Research Reactor Institute, Kyoto University

INTRODUCTION: It is well known that dielectric materials such as natural quartz exposed to ionizing radiation emit thermoluminescence (TL) and optically stimulated luminescence (OSL). OSL is a well-established tool for measuring radiation doses in unfired sediments [1]. It has features in common with TL which has long been used in measuring radiation doses [2]. Both TL and OSL dosimetry with white mineral do not need to be specially installed in advance, prior to dose estimation.

Quartz is an excellent material for use in dosimetry, because of its almost ubiquitous availability including an accidental place. Feldspar is an extensive ternary family of minerals appropriate for OSL and TL dosimetry as they display a strong luminescence and are quite common in the Earth's formation, although it has anomalous fading effects which could decay OSL-related luminescence signals.

However, the detailed emission mechanisms of TL and OSL from natural minerals such as quartz and feldspar are not yet clear. In this study, the emission mechanisms of TL and OSL were investigated in conjunction with various radiation-induced phenomena after annealing treatments of quartz samples, involving TL, OSL and electron spin resonance (ESR) measurements.

EXPERIMENTS: Natural quartz were sieved to adjust the grain sizes ranging from 150 – 250 μm in a diameter after extracted from surface soil with conventional method [3]. The quartz samples were annealed at 800 ºC for 24 hours in an electric furnace, to make luminescence signals strong. In addition, one part of the annealed quartz samples were treated with supercritical water. Both of the annealed and the treated samples were irradiated a dose of 20 kGy with ^{60}Co source (10.09 kGy/h at center position) at liquid nitrogen temperature at Kyoto University Research Reactor Institute (KURRI). The irradiated samples were measured by an ESR spectrometer (Jeol Ltd., JES-TE 200) at −196 ºC. All preparations were carried out under dim red light.

After the ESR measurements, all samples were kept to measure luminescence signals in a dark room. TL (Red-TL and Ultraviolet-TL) and OSL were measured by a JREC automated TL/OSL-reader system.

RESULTS: The ESR signals of Al centers as hole-trapped centers and Ti centers ($[TiO_4/H^+]^0$, $[TiO_4/Li^+]^0$ and $[TiO_4/Na^+]^0$) as electron-trapped centers were detected in the annealed and treated quartz samples as before. Both signals showed similar shapes. Moreover, in ESR spectra of the treated sample sampled in one point, small two signals caused by atomic hydrogen were found. However, this signals should be confirmed the reproducibility at future experiment.

The OSL signals were measured at three times for each sample. The OSL decay curves of both samples had similar shapes but different intensities corrected by each sample weight. The OSL intensity of the treated sample was higher than the OSL intensity of the annealed sample. From the result, OSL intensity could be increased by the supercritical water reaction.

The Ultraviolet-TL (UVTL) signals were measured at three times for each sample. The UVTL glow curves of both samples had similar shapes but different intensities corrected by each sample weight. The UVTL intensity of the annealed sample was higher than the UVTL intensity of the treated sample. From the result, UVTL intensity could be decreased by the supercritical water reaction but as opposite effect comparing with the OSL.

The Red-TL (RTL) signals were measured at three times for each sample. The RTL glow curves of both samples had similar shapes and similar intensities corrected by each sample weight. From the result, RTL intensity could not be influenced by the supercritical water reaction.

The results of ESR, OSL, UVTL and RTL were not difference between quartz samples collected at two places.

In this research, the luminescence emission mechanism could not be identified.

Second experiment was scheduled in February of 2018 but was canceled by preparation of personnel changes. Therefore, during the Visiting Researchers Program an experiment was done using Co-60 Gamma-ray Irradiation Facility.

REFERENCES:

[1] Huntley, D. J., *et al.*, Nature, **313** (1985) 105-107 .
[2] Mckeever, S. W. S., Cambridge University Press, Cambridge, (1985) 103-105.
[3] Fujita, H., *et al.*, Radiat. Meas., **46** (2011) 565-572.

CO5-10 Trace Amounts of Halogens (Cl, Br and I) in Andesite and Basalt Reference Materials

S. Sekimoto, N. Shirai[1] and M. Ebihara[1]

Research Reactor Institute, Kyoto University

[1]Graduate School of Science, Tokyo Metropolitan University

INTRODUCTION: Accurate and reliable data of halogen abundance have been rarely reported for terrestrial samples, such as andesite and basalt materials. Since halogens differ in volatility from element to element, their content and relative abundance are highly informative when discussing the petrogenesis of such samples. Recently, we have improved the radiochemical neutron activation analysis (RNAA) procedure for trace amounts of halogens (Cl, Br and I) [1]. In this study, our RNAA was applied to one andesite and three basalts materials that are available in U.S. Geological Survey (USGS) and then, our RNAA values were compared with the literature values.

EXPERIMENTS: Trace amounts of Cl, Br and I in the one andesite (AGV-2) and three basalts (BCR-2, BHVO-2, and BIR-1a) were determined by RNAA. The RNAA procedure is described elsewhere [1-2]. Those samples were repeatedly analyzed more than two times.

Table 1: Cl, Br and I contents in USGS andesite and basalts materials analyzed by RNAA in this study and from the Literature

([a] Not reported. [b] Number of analysis was two. [c] IC (Ion chromatography) and ICPMS were coupled with pyrohydrolysis. [d] Analytical methods for individual data were Spark-source Mass Spectrometry, Neutron Activation Analysis, Ion Selective Electrodes, Ion Chromatography, *etc*.)

Sample	Cl (mg kg^{-1})	Br (mg kg^{-1})	I (mg kg^{-1})	Method [c]	Ref.
AGV-2	**72.8 ± 2.7**	**0.101 ± 0.007**	**0.197 ± 0.038**	**RNAA**	[2]
	75 ± 3	- [a]	-	IC	[3]
	-	0.107-0.145 [b]	0.007 ± 0.001	ICP-MS	[3]
	61 ± 3	-	-	IC	[4]
BCR-2	**112 ± 1**	**0.144 ± 0.008**	**0.082 ± 0.022**	**RNAA**	[2]
	98 ± 8	-	-	IC	[3]
	-	0.157-0.175 [b]	0.017 ± 0.004	ICP-MS	[3]
	89 ± 6	-	-	IC	[4]
	101	-	-	XRF	[5]
BHVO-2	**104 ± 4**	**0.240 ± 0.013**	**0.307 ± 0.050**	**RNAA**	[2]
	150 ± 21	-	-	IC	[3]
	-	0.269-0.277 [b]	0.016 ± 0.002	ICP-MS	[3]
	81 ± 11	-	-	IC	[6]
	-	0.29 ± 0.10	0.020 ± 0.012	ICP-MS	[6]
	89 ± 7	-	-	IC	[4]
BIR-1a	**5.64 ± 0.43**	**0.039 ± 0.012**	**0.041 ± 0.009**	**RNAA**	[2]
BIR-1	*26 ± 6*	*<2*	-	*Compiled values* [d]	[7]
	44	-	-	IC	[3]
	-	0.065 ± 0.026	0.014 ± 0.002	ICP-MS	[3]

RESULTS: Our RNAA data for AGV-2, BCR-2, BHVO-2, and BIR-1a were consistent with previously published data for Cl and Br but not for I [3, 4, 6]. Iodine values measured by RNAA for these reference materials (RM) are higher by factors of 3 to 10 compared those measured by pyrohydrolysis and ICP-MS analysis. We suggest that I may be partially lost during slow evaporation and concentration of pyrohydrolysis solutions prior to mass spectrometry. From a detailed comparison in Cl values between RNAA and IC coupled with pyrohydrolysis, it can also be seen that IC values tend to be lower than the RNAA values (Fig. 1), because Cl may not always be quantitatively extracted from basaltic and andesitic RM during pyrohydrolysis. Sekimoto and Ebihara (2013) reported similar discrepancies for Br and I in sedimentary RM.

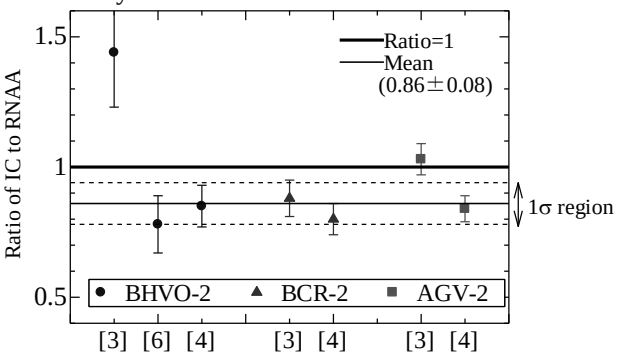

Fig. 1. Concentration ratios of Cl between RNAA values and IC values.

REFERENCES:

[1] S. Sekimoto and M. Ebihara, Anal. Chem., **85** (2013) 6336-6341.

[2] S. Sekimoto and M. Ebihara, Geostand, Geoanal. Res., **41** (2017) 213-219.

[3] A. Michel and B. Villemant, Geostand. Newslett., **27** (2003) 163-171.

[4] Q. Wang *et al.* Geostand. Geoanal. Res., **34** (2010) 175-183.

[5] D. Hanano *et al.* Geochem. Geophy. Geosy., **11** (2010) Q01004, 1-22.

[6] H. Balcone-Boissard *et al.* Geostand. Geoanal. Res., **33** (2009) 477-485.

[7] E.S. Gladney and I. Roelandts, Geostand. Newslett., **12** (1988) 63-118.

CO5-11 Application of Neutron Activation Analysis to Micro Gram Scale of Solid Samples

S. Sekimoto, N. Shirai[1] and M. Ebihara[1]

Research Reactor Institute, Kyoto University

[1] Graduate School of Science, Tokyo Metropolitan University

INTRODUCTION: Instrumental neutron activation analysis (INAA) is often used in cosmochemistry, where meteorites are the objects for INAA. Chondritic meteorites (chondrites) and iron meteorites contain relatively high contents of Co and Ir compared with those in the earth crust. As Co and Ir have high sensitivity in INAA, they can be good markers for the identification of such extraterrestrial materials. In NAA of chondrites, a few tens mg of specimen is commonly used. For such a case, a few hundred μg kg^{-1} of Ir and a few hundred mg kg^{-1} of Co can be reliably determined. When an extremely small size (e.g., micro gram) of samples such as micrometeorites recovered on the Earth surface and tiny particles returned from extraterrestrial asteroids are to be analyzed by INAA, the conventional INAA procedure used for a few tens mg is not suitable. For such tiny samples, neutron irradiation with high neutron flux and long irradiation time (namely, high neutron dose) is required. Recently we have presented the INAA procedure for micro gram scale of solid samples [1]. In this report, one typical example for the application of the proposed procedure is shown with limited scientific discussion. For the meteoritic grain sample, here, a chunk of the Kilabo (LL6) chondrite was crushed and a single piece was picked.

RESULTS: Instrumental NAA results of the Kilabo piece are summarized in Table 1. Since the weight of this piece is less than 1 mg and cannot be weighed, elemental concentrations are not given.

The Kilabo sample analyzed in this study is a small silicate piece. Therefore, its chemical composition cannot be the same as that of the bulk Kilabo meteorite. As no mineralogical and petrological information is available for the Kilabo piece sample, the detailed cosmochemical discussion cannot be developed. Here, only Ni and Co contents are concerned. Cobalt and Ni are known to behave similarly cosmochemically [2] as well as geochemically. Both elements tend to be hosted in metals in ordinary chondrites like Kilabo. Figure 1 shows the relationship between Co/Fe and Ni/Fe ratios for the Kilabo piece. In addition, data for CI chondrite [3], LL6 chondrite (bulk) [4] and metal separate of LL6 and L6 chondrites [5] are also shown for comparison. The solid line represents the Co/Ni ratio of CI chondrite, on which the Kilabo piece sample is placed along with LL6 bulk and metal samples. This suggests that the Kilabo piece contains a tiny metal grain inside. A similar chemical characteristic was observed in tiny silicate grains recovered from the asteroid Itokawa by the Hayabusa spacecraft [6]. Their Co/Fe and Ni/Fe ratios are similar to those of the Kilabo piece, falling on the CI line as seen in Fig. 1.

As the Co/Ni ratio in the Kilabo piece is chondritic, the kilabo piece might contain 0.5-0.6 pg of Ir if we assume that the Ir/Co and Ir/Ni ratios in the Kilabo piece are equal to those in CI chondrite [3]. Although only an upper limit was derived for the Kilabo piece, it is clear that Ir is depleted in the tiny metal grain that the Kilabo piece contains. From the view point of Ir-depletion, Kilabo and Itokawa grains thus appear alike.

Table 1 Elemental contents in Kilabo

Sm	0.38 ± 0.04 pg	Cr	4.60 ± 0.04 ng
La	2.6 ± 0.3 pg	Ni	14.5 ± 0.3 ng
Sc	22.2 ± 0.4 pg	Au	0.62 ± 0.03 pg
Fe	0.576 ± 0.007 μg	Zn	1.4 ± 0.1 ng
Na	7.93 ± 0.12 ng	Ir	< 0.068 pg
Co	0.589 ± 0.008 ng		

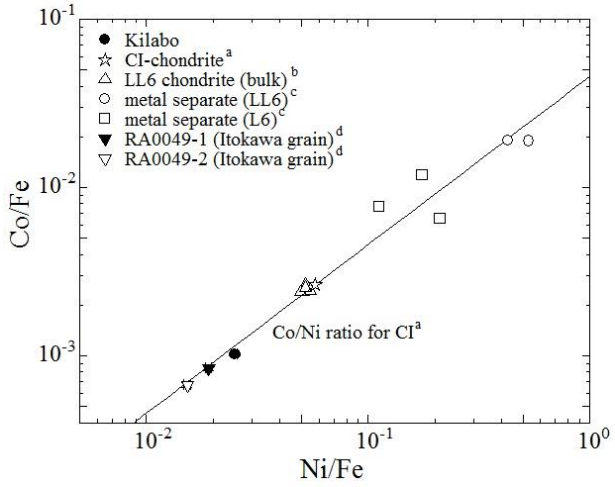

Fig. 1. Correlation between Co/Fe and Ni/Fe ratios in several astromaterials ([a] [3]. [b] [4]. [c] [5]. [d] [6])

REFERENCES:

[1] S. Sekimoto *et al.,* J Radioanal Nucl Chem., **307** (2016) 1757-1764.

[2] J.T. Wasson Meteorites-Their Record of Early Solar-System History, W. H Freeman and Company, New York (1985).

[3] E. Anders & N. Grevesse, Geochim Cosmochim Acta., **53** (1989) 197–214.

[4] G.W. Kallemeyn *et al.,* Geochim Cosmochim Acta., **53** (1989) 2747-2767.

[5] P. Kong & M. Ebihara, Geochim Cosmochim Acta., **61** (1997) 2317-2329.

[6] M. Ebihara *et al.,* Science, **333** (2011) 1119-1121.

CO5-12 Comparison of Extractable Organochlorine and Organobromine Speciated by Molecular Weight in Various Environmental Matirices

K. Mukai, T. Fujimori, K. Oshita, S. Fukutani[1] and S. Takahashi[2]

Department of Environmental Engineering, Graduate School of Engineering, Kyoto University
[1] Research Reactor Institute, Kyoto University (KURRI)
[2] Graduate School of Agriculture, Ehime University

INTRODUCTION: Studies on extractable organohalogens (EOX, X=Cl, Br) have indicated that there are many unidentified organochlorine/bromine compounds (OHCs) in the environment [1, 2]. Some of these unidentified compounds have bioaccumulation potential and toxicity like persistent organic pollutants (POPs), but little is known about how much of EOX can have POP-like properties and which environment is an important source or sink of unidentified POP-like OHCs. In general, molecular weights of POP-like OHCs are below 1000. Thus, EOX in this fraction can be indicator for potential amounts of POP-like OHCs.

In this study, we used gel permeation chromatography (GPC) to separate EOX into low-molecular-weight EOX (EOX-L) and high-molecular-weight EOX (EOX-H). We compare the results in various samples and discuss which environment has high potential of POP-like OHCs including unidentified compounds.

EXPERIMENTS: Natural forest soils are collected from O, A, B layers at Mt. Yatsugatake and Tango Peninsula in Kyoto. Soil standard samples are taken from The Japan Society for Analytical Chemistry (JSAC) standard reference material 0422 (0–3 cm depth) and 0421 (3–10 cm depth). They are both collected at forest near a manicipal solid waste incinerator (MSWI). Sediment and Finless porpoise blubber were samples studied in previous studies [3, 4]. House dust came from the NIST standard reference materials 2585. Urban particulate matter is taken from the NIST standard reference material 1648a. MSWI bottom ash and MSWI fly ash was taken from the JSAC standard reference materials 0512 and 0511 respectively.

Samples (5 g for soils and sediment, 2 g for house dust, ash and blubber, 0.5 g for urban particulate matter) were extracted by ultra-sonic extraction method using three different solvents; acetone/hexane (1:1) 10 mL, hexane 10 mL and toluene 10 mL. Three fractions were combined and reduced to 10 mL by rotary evaporation followed by washing for inorganic Cl and Br removal. Then extracts were applied to GPC. The first fraction is EOX-H and the second fraction is EOX-L. Each fraction was used for neutron activation analysis. 2 mL was put in a polyethylene (PE) bag and dried up under normal temperature and pressure. Samples were irradiated for 5 min with a thermal neutron flux of 2.0–2.4×1013 cm^{-2} · S^{-1} at KURRI. ^{38}Cl ($t_{1/2}$ = 37.18 min, E_γ = 1642, 2168 keV) and ^{80}Br ($t_{1/2}$ = 17.6 min, Eγ = 616 keV) were measured by using a Ge semiconductor detector for 60 s.

RESULTS: Results are shown in Fig. 1. In order to evaluate the POP-like potencies, we focus on EOX-L below. Comparing to the natural forest soil, EOCl-L is similar in soils and sediment, while EOBr-L is 3.6 times higher in sediment. This indicates that the sediment is contaminated by synthetic brominated compounds from industries. EOCl-L in house dust, and ash samples are about 2–3 times higher, and EOBr-L in house dust is 47-fold higher than those of forest soils. In finless porpoise blubber, EOCl-L is 6.7 times higher and EOBr-L is 17 times higher than natural forest soil. This is explained by the bioaccumulation properties of POP-like OHCs. In urban particulate matter, even higher concentrations of EOX-L are observed; 27 times higher EOCl-L and 112 times higher EOBr-L (compared to natural forest soil), suggesting that urban particulate matter is extremely important reservoir of OHCs.

We showed the potential of POP-like organochlorine compounds are high in urban particulate matter, house dust, fly ash, and finless porpoise blubber; and the potential of POP-like organobromine compounds is high in sediment, urban particulate matter, house dust, and finless porpoise blubber. Further researches are expected toward these environmental matrices.

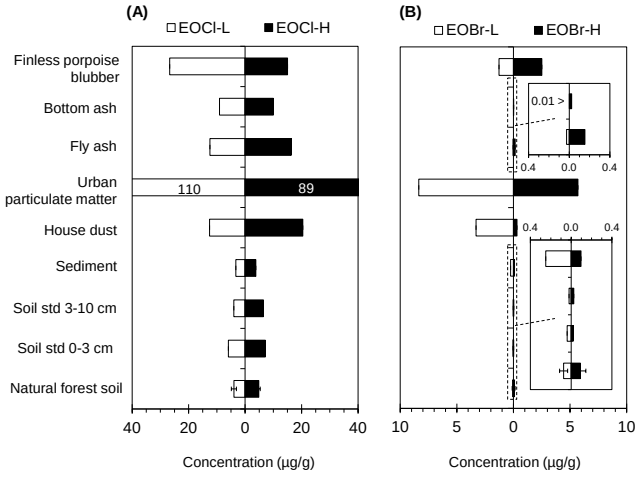

Fig. 1. (A) Concentrations of EOCl-L and EOCl-H. (B) Concentrations of EOBr-L and EOBr-H.

REFERENCES:

[1] K. Kannan *et al*., Environ. Sci. Technol., **33** (1999) 1004-1008. 7.
[2] Y. Wan *et al*., Environ. Sci. Technol., **44** (2010) 6068-6073. 16.
[3] S. Takahashi *et al*., Chemosphere., **64** (2006) 234-244. 2.
[4] S. Takahashi *et al*., Organohalogen Cmpds. **67** (2005) 430-433.

CO5-13 Chemical Compositions of Chromitite Reference Materials (CHR-Bkg and CHR-Pt+)

N. Shirai, S. Sekimoto[1] and M. Ebihara

Department of Chemistry, Tokyo Metropolitan University

[1]Institute for Integrated Radiation and Nuclear Science, Kyoto University

INTRODUCTION: Chromitite is mostly composed of chromite ($FeCr_2O_4$), which plays an important role for behavior of PGE during igneous processes [e.g., 1]. Ultramafic and mafic samples have positive correlations between Cr, and Os, Ir and Ru, implying that these four elements are partitioned into the same minerals [1]. Partition coefficients of Os, Ir and Ru between chromite and silicate melt are higher than those of Rh, Pd and Pt [2]. As chromite is known to be resistant to most acid, complete digestion of rock samples including chromite is essential for reliable determination of PGE when analytical methods accompanying acid digestion such as ICP-MS. It has been getting common to use ICP-MS for the determination of PGE in rock samples. The commonly used digestion techniques are NiS fire-assay and acid digestion in Carius tube and a high pressure asher (HPA-S) for the determination of PGE in rock samples. A major concern in ICP-MS of PGE in rock samples has been whether NiS fire-assay can completely dissolve chromite or not. Komatiite samples were analyzed by both NiS fire-assay and Carius tube digestion and it was found that PGE values obtained from NiS fire-assay are systematically lower than those from Carius tube digestion [2]. In the later studies, komatiite samples were analyzed by using both NiS fire-assay and acid digestion in Carius tube or HPA-S, and it was demonstrated that two analytical results are not distinguishable from each other [3]. In the previous studies [2,3], different samples of different amounts were analyzed. In the comparison of the two analytical results, the sampling bias could become a critical problem. Therefore, the same samples of GPt-5 were analyzed by using different analytical methods (INAA and NiS fire-assay combined with ICP-MS) in order to solve the sampling bias problem [4]. Iridium was determined by INAA, while Ru, Rh, Pd, Ir and Pt values were obtained by using INAA. Iridium values obtained by INAA and ICP-MS were consistent with each other and it was concluded that NiS fire-assay can completely digest chromite. Other chromitite reference materials (CHR-Bkg and CHR-Pt+) are analyzed in order to obtain a additional evidence whose NiS fire-assay can release all PGE from chromite. In this paper, INAA results are presented.

EXPERIMENTS: Two chromitite reference samples (CHR-Bkg and CHR-Pt+) were analyzed by INAA. Neutron irradiation was performed in Institute for Integrated Radiation and Nuclear Science, Kyoto University. The Sc, Cr, Fe, Co, Ni, Zn and Ir concentrations were determined after the 4 h irradiation. For quantification, JB-1a, a basaltic geochemical reference powder issued by the Geological Survey of Japan, was used as a calibration standard. Literature values of Jochum et al. [5] were used. In addition, the Smithsonian Institution Allende meteorite powder and Ir-doped filter paper were irradiated for the determination of the Ni and Ir concentrations. The Ni value of the Smithsonian Institution Allende meteorite powder was taken from Kallemeyn and Wasson [6] and Kallemeyn et al. [7].

RESULTS: The measurement results of CHR-Pt+ and CHR-Bkg are summarized in Table 1. Mean values and relative standard deviations (RSDs) along with the literature values [8] are also shown. Our mean values for CHR-Pt+ and CHR-Bkg are consistent with literature values [8] within 15%. It is noted that there is a large variation of Ir values (RSD; 50%) in CHR-Bkg. This large variation of 50% for Ir is due to the sample heterogeneity. In consideration that RSD for other elements are less than 3%, it is likely that Ir alloy or PGE alloy are heterogeneously distributed in CHR-Bkg.

REFERENCES:

[1] P. Page *et al.*, Chem. Geol., **302-303** (2001) 3-15.

[2] I. S. Puchtel and M. Humayun, Geochim. Cosmochim. Acta, **65** (2001) 2979-2993.

[3] D. Savard *et al.*, Geostand. Geoanal. Res., **34** (2010) 281-291.

[4] R. Akhter *et al.*, Geochem. J., **50** (2016) 179-185.

[5] K. P. Jochum *et al.*, Geostand. Geoanal. Res., **40** (2016) 333-350.

[6] G. W. Kallemeyn and J. T. Wasson, Geochim. Cosmochim. Acta, **45** (1981) 1217-1230.

[7] G. W. Kallemeyn *et al.*, Geochim. Cosmochim. Acta, **53** (1986) 2747-2767.

[8] K. Govindaraju, Geostand. Newslett., **18** (1994) 1-158.

Table 1. Measurements results for three CHR-Pt+ (A-C) and CHR-Bkg (D-F) samples obtained by INAA.

Element	Unit	CHR-Pt+						CHR-Bkg					
		This work[a]					Literature	This work[a]					Literature
		A	B	C	Mean[b]	RSD[c]	value[d]	D	E	F	Mean[b]	RSD[c]	value[d]
Sample mass	mg	53.5	52.1	49.3				64.0	55.8	65.2			
Sc	ppm	3.81±0.03	3.84±0.03	3.81±0.03	3.82±0.02	0.5		5.57±0.02	5.46±0.02	5.37±0.02	5.47±0.10	1.8	
Cr	%	11.8±0.2	12.1±0.2	11.9±0.2	11.9±0.1	1.2	13.91	18.7±0.3	18.1±0.3	17.9±0.3	18.2±0.4	2.1	19.88
Fe	%	8.56±0.08	8.73±0.09	8.48±0.09	8.59±0.13	1.5	9.379	9.62±0.08	9.33±0.08	9.26±0.08	9.40±0.19	2.0	9.701
Co	ppm	185±2	190±2	186±2	187±2	1.3	177	192±1	186±1	185±1	188±4	2.1	167
Ni	ppm	5310±40	5540±40	5190±40	5340±180	3.3	5862	1830±10	1750±20	1760±10	1780±40	2.2	2006
Zn	ppm	205±7	214±8	216±8	212±6	2.8	192	234±7	229±7	231±7	231±2	1.0	205
Ir	ppb	5690±40	5940±40	6770±50	6130±570	9.3	6200	43.6±1.7	100±3	46.7±2.1	63.4±31.7	50	28

[a]Errors quoted for A to F are due to counting statistics (1 s) in gamma-ray spectrometry.

[b]Mean values of replicate analyses with their standard deviations (1s).

[c]Relative standard deviations (in % for 1 s).

[d]Govindaraju (1994).

CO5-14 Fission Track Dating and Thermal History of Hydrothermally Altered Rock Sample

H. Ohira and A. Takasu

Department of Geoscience, Shimane University

INTRODUCTION: Fission track (FT) dating was carried out to estimate ages and cooling history of hydrothermally altered rock sample from the Tsuchihashi mine, Bizen City, Okayama Prefecture. The mine yields high grade clay minerals used as raw materials for refractories and ceramics. Original rock of the mine is Cretaceous pyroclastic rock, and is thought to be strongly altered to form clay deposit, by hydrothermal activity following the eruption of pyroclastic rocks and Caldera Formation. In the mine area, several clay zones such as pyrophyllite, sericite and kaolinite, develops in response to conditions of hydrothermal fluid infiltrated [1]. Sericite vein sample which develops in sericite ore zone was collected. Occurrence of the vein implies the vein formed at the latest stage of hydrothermal activity. The depositional age of the original pyroclastic rock is thought to be 82.4±0.6Ma by U-Pb zircon dating [1], and the period of hydrothermal activity is estimated by K-Ar dating for clayey rock samples (74.2±1.8M ~ 77.8±1.7Ma) [2].

EXPERIMENTS: Rock sample was crashed, sieved and fraction less than 0.3mm in grain size was separated. Heavy minerals were concentrated using conventional method of heavy liquid and magnetic separator. Zircons were mounted in PFA Teflon, and then polished to reveal a complete internal surface, and was etched in a NaOH-KOH eutectic melt at 225˚C [3] for 13-17 hours. Samples were irradiated at pneumatic tube of graphite facility (Tc-pn) of Kyoto University Reactor (KUR). After irradiation, external detectors (mica) were etched in 46% HF at 25˚C for 6-7 minutes (for mineral mounts) and for 20-50min (for NIST-SRM612 glass). FT density was measured at 1000× magnification with a dry objective.

RESULTS: Despite of more than 150 grains used for experiments, almost grains were uncountable because of its significantly high spontaneous track density. Instead, only 24 grains which show clearly visible tracks due to relatively lower FT density were successfully measured. FT age was 74.1±2.5Ma. The obtained FT age is nearly 8Ma younger than U-Pb age previously reported (82.4±0.6M [1]). The discordant between the two ages is probably attributable to the difference of closure temperature of each dating method. Closure temperature of U-Pb and FT methods are thought to be 800℃< [4] and 230℃< [5], respectively. The FT age from the sericite vein is probably indicates the period when the sericite vein formed by hydrothermal activity, and then cooled below 230℃during the latest cooling stage. Fluid inclusion data of secondary inclusion arrays in quartz phenocryst from the mine show relatively wide range of homogenization temperature (270~310℃), suggesting that the temperature condition of hydrothermal alteration was completely exceeded the closure temperature of FT dating method. Assuming that the hydrothermal activity began immediately after the deposition of original pyroclastic rock and continued to form the sericite vein, the gap of ages (nearly 8Ma) may indicate the duration of hydrothermal fluid circulation following volcanic activity of this area.

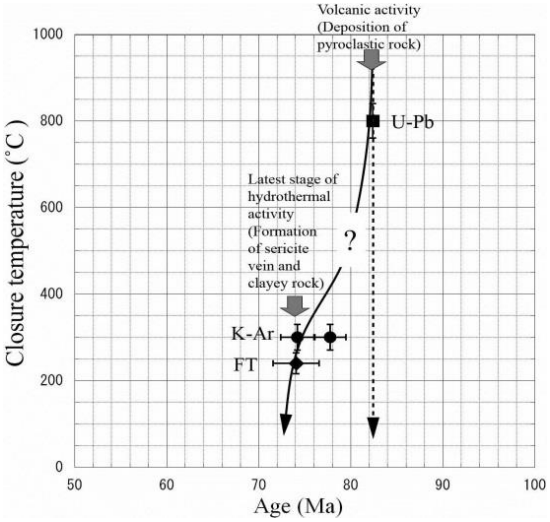

Fig.1 Preliminary estimated cooling history (solid line) of hydrothermally altered rock sample (sericite vein), from the Tsuchihashi mine.

[1] Sato D., Yamamoto T. and Takagi T., 2016, Geology of the Banshu-Ako district. Quadrangle Series, 1:50000, Geological Survey of Japan, AIST, 68p (in Japanese with English abstract).
[2] Motomiya H., Kitagawa R. and Nishido H., 2000, Clay Science (Nendo Kagaku) **40**, 46-53.
[3] Gleadow A.J.W. *et al.*, 1976, Earth and Planetary Science Letter, **33**, 273-276.
[4] Cherniak, D.J. and Watson, E.B., 2000, Chemical. Geology, 172, 5–24.
[5] Hasebe N. and Tagami T., 2001, Tectonophysics **331**, 247-267.

CO5-15 Thermal History of Precambrian Metamorphic Rocks

H. Hyodo[1], K. Sato[2] and H. Kumagai[3]

[1]*Research Institute of Natural Sciences, Okayama University of Science*
[2]*Department of Applied Chemistry and Biochemistry, National Institute of Technology, Fukushima College*
[3] *Research Center for Marine Resources, Japan Agency for Marine-Earth Science and Technology*

INTRODUCTION: Acasta gneiss is known as the oldest rock (ca. 4.0 Ga) by U-Pb zircon SHRIMP dating [1]. The thermal history of the rock seems to be complicated [2] because it shows much younger age (1.9 Ga) in apatite U-Pb method [3], hornblende and biotite in K-Ar method (unpublished results).

K-Ar system is more susceptive to external disturbance compared to U-Pb system. On the other hand, if a zircon grain acts as a solid guard for its inclusions against such disturbance, the inclusions may keep the primary K-Ar system when they are formed, and may provide some insights on the precambiran atmosphere. Variety of inclusions might behave separately, but average behavior could be determined from the experiment. Several zircon grains from Acasta gneiss were selected to determine the $^{40}Ar/^{39}Ar$ age of such inclusions.

EXPERIMENTS: Experimental procedure is the same as described as previous studies on single grain datings. Rock samples were crushed, and sieved in #25-100 mesh. After ultrasonic cleaning in distilled water, single mineral grains were handpicked. The zircon grains were irradiated in the KUR for 22 hours at 1 MW and subsequently 6 hours at 5MW. The total neutron flux was monitored by 3gr hornblende age standard [4], [5], which was irradiated in the same sample holder. In the same batch, $CaSi_2$ and $KAlSi_3O_8$ salts were used for interfering isotope correction. A typical J-value was $(1.183 \pm 0.009) X10^{-2}$. In stepwise heating experiment, temperature of a mineral grain was measured using infrared thermometer whose spatial resolution is 0.3 mm in diameter with a precision of 5 degrees. The amount of argon isotopes in inclusions seems to be small. In some cases when grain sizes are too small for the analyses, mutiple (3-5) grains were heated under defocused beam in order to increase the sample size. Extracted argon isotopes were measured using the custom made mass spectrometer [5].

RESULTS: One of $^{40}Ar/^{39}Ar$ age spectra of zircon grains were illustrated in Fig. 1. Since the average grains sizes are nomally 100-200 microns, four grains were heated together. The temperature control was difficult for the milky to transparent grains particularly at higher temperatures. The laser power was increased rapidly above 800 degrees to fuse the grain. The grains do not release much argon isotopes below 1000 degrees in most cases. This behavior suggests heat resistant nature of the zircon

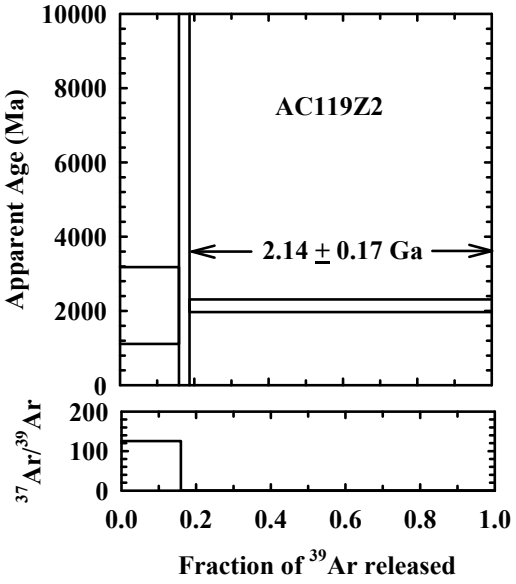

Fig. 1. $^{40}Ar/^{39}Ar$ age spectra of zircon from Acasta gneiss. The error seems to be large due to the small amount of 39Ar, but it indicates an age close to the age reported from other potassium minerals.

grains. The plateaue age obtained here are slightly older than the average age of hornblende and biotite in the Acasta gneiss, but apparently much younger than the U-Pb age. The similar behavior is confirmed in another sample. This seems to be consistent in terms of closure temperature if we assume that closure temperature of potassium minerals in the zircon is higher than those of hornblende and biotite. The number of analyses is too few to make a solid conclusion, but the results suggest that the Acasta gneiss suffered from relatively high temperature metamorphism above 500°C.

Inclusions in the zircon possibly have a variety of mixture including fluid inclusion and initial argon from the ancient environment. It is impossible to separate each contribution, but the average behavior seems to give consistent results.

REFERENCES:

[1] S.A.Bowring and I.S. Williams, *Contributions to Mineralogy and Petrology*, **134** (1999) 3–16.
[2] T. Iizuka *et al. Precambrian Research* **153** 179-208.(2007).
[3] Y. Sano, *et al. Geochimica Cosmochimica Acta* **63** (1999) 899–905.
[4] J.C. Roddick, *Geochim. Cosmochim. Acta* **47** (1983) 887-898.
[5] H. Hyodo, *Gondwana Research* **14** (2008) 609-616.

CO5-16 Applicability Verification of Isotopic Analysis of Cs by TIMS

Y. Shibahara, S. Fukutani, T. Kubota, T. Shibata[1], M. Yoshikawa[2]

Research Reactor Institute, Kyoto University
[1]Graduate School of Science, Hiroshima University
[2]Institute for Geothermal Sciences, Kyoto University

INTRODUCTION: For the analysis of radionuclide which was released on the accident of Fukushima Dai-ichi Nuclear Power Plant, we have studied the applicability of the mass spectrometry, especially thermal ionization mass spectrometry (TIMS). Our study has focused on Cs, Sr, U and Pu as target of the analysis by TIMS. In this study, we discussed the applicability of the isotopic analysis of Cs by the comparison of our results with the literature data.

EXPERIMENTS: Cs was recovered from the standard reference materials of IAEA-373 and IAEA-156, the environmental sample obtained in Fukushima prefecture and the natural uranium irradiated at KUR. The standard reference materials are the environmental samples contaminated by the accident of Chernobyl Nuclear Power Plant. The ^{137}Cs concentration of them corrected on 11 Mar 2011 was 2.4×10^{-12} g/g for IAEA-373 and 4.7×10^{-14} g/g for IAEA-156 respectively. The concentration of ^{137}Cs of the environmental sample obtained in Fukushima prefecture was about 2.6×10^{-10} g/g (corrected on 11 Mar 2011). The irradiation of the natural uranium (10 mg) was performed with the neutron flux of 5.5×10^{12} n/s cm^2 and the irradiation time of 3 hours. By using ORIGEN-II code [4], the amount of the ^{137}Cs generated by this irradiation was estimated at 7.4×10^{-11} g. Cs was recovered according to the recovery scheme [1-3]. After the preparation of the samples for the isotopic ratio analysis of Cs, the Cs isotopic ratio (= ^{135}Cs/^{137}Cs) was analyzed by TIMS.

In the analysis of Cs by TIMS, a thermal ionization mass spectrometer (TRITON-T1, Thermo Fisher Scientific) with a rhenium single filament system was used. The Cs sample prepared for the TIMS analysis was loaded onto a rhenium filament with a TaO activator. Because of the loading amount of Cs (max. 1×10^{-12} g), the mass spectrometry was conducted with a secondary electron multiplier detector and the peak jump method [1-3].

RESULTS: Figure 1 shows the mass spectra of Cs recovered from the standard reference material of IAEA-373 and the environmental sample obtained in Fukushima prefecture. We found the clear difference in the beam intensity of ^{135}Cs compared with that of ^{137}Cs. We obtained the ^{135}Cs/^{137}Cs ratio of *ca*. 0.50 for the standard reference material of IAEA-373, and *ca*. 0.36 for the environmental sample obtained in Fukushima prefecture: these values are corrected on 11 Mar. 2011.

Figure 2 shows the comparison of the ^{135}Cs/^{137}Cs ratio observed in our study with that of the literature data for the sample of IAEA-156 and the environmental sample

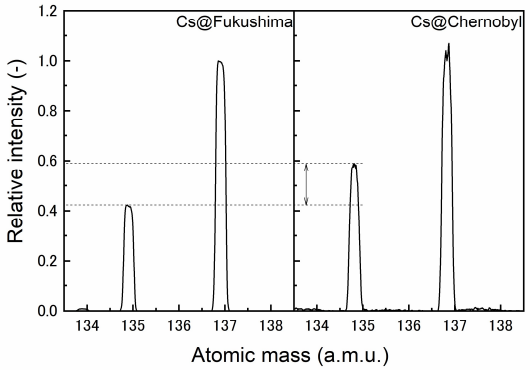

Fig. 1 Mass spectra of Cs recovered from environmental sample. Cs@Fukushima: Cs was recovered from the environmental sample obtained Fukushima prefecture. Cs@Chernobyl: Cs was recovered from standard sample of IAEA-373.

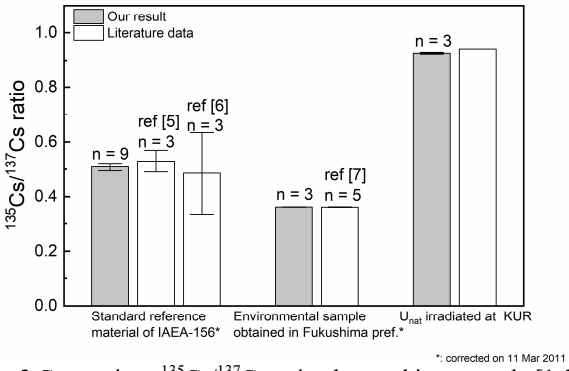

Fig. 2 Comparison ^{135}Cs/^{137}Cs ratio observed in our study [1-3] and literature data [5-7]. Error bar means ±2σ.

[5-7] and the calculation results by using the ORIGEN-II code for the sample recovered from the irradiated uranium [4]. Although the statistical precision was not excellent because of the low concentration of the radioactive Cs in the environmental sample, we found that the ^{135}Cs/^{137}Cs ratio observed in our study shows the agreement with the literature data and also shows the linear correlation with the literature data as follows;

$Y = (1.00\pm0.01)\times X$, $R^2 = 1.000$ or

$Y = (-0.01\pm0.01) + (1.03\pm0.04)\times X$, $R^2 = 1.000$.

where X and Y mean the isotopic ratio of ^{135}Cs/^{137}Cs of our study and the literature data, respectively.

REFERENCES:

[1] Y. Shibahara *et al.* J. Nucl. Sci. Technol. 2014, 51, 575-579.
[2] Y. Shibahara *et al.* Radiological issues for Fukushima's revitalized future. Springer. 2016. 33-46.
[3] Y. Shibahara *et al.* J. Nucl. Sci. Technol. 2017, 54, 158-166.
[4] S. B. Ludwig *et al.* ORNL/TM-11018. ORNL. 1989.
[5] M. S. Snow *et al.* J. Environ. Radioact. 2016, 151, 258-263.
[6] J. Zheng *et al.* Anal. Chem. 2016, 88, 8772-8779.
[7] J. A. Dunne *et al.* Talanta. 2017, 174, 347-356.

CO5-17 Characteristics of Calcite Thermoluminescence and Its Use for Age Estimate

N. Hasebe, K. Miura[1], M. Ogata, U. Uyangaa[1], K. Kinugawa[1] and R.Hayasaka[1]

Institute of Nature and Environmental Technology, Kanazawa University
[1]Graduate School of Natural Science and Technology, Kanazawa University

INTRODUCTION: Luminescence dating observes the natural accumulated radiation damage caused by radioisotopes such as U and Th as the form of glow after stimulation by heating or lightening. Thermally stimulated luminescence from calcite shows strong red emission. When thermoluminescence (TL) characteristics of calcites are examined using both of natural occurring and synthetic calcite, their response to the various radiations depends on minor chemistry (Fe, Mg, Mn and Sr). After establishment of empirical relationship between impurity concentration and luminescence efficiency for each radiation, the calcite collected from Philippines was dated.

EXPERIMENTS: First, the mineral species of the samples were examined by XRD measurement and it turned out to be calcite. Then luminescence emission from calcite was measured by the luminescence reader MOSL-22, and dose was estimated by the external x-ray source, whose dose rate is calibrated as 0.1 Gy/sec with quartz. The glow curve was compared to that of calcite from other origin. Chemical compositions were measured by LAICPMS to estimate annual dose and luminescence efficiencies.

RESULTS: The emission curve shows high emission at around 360 ℃, and the response to radiation is small (or insignificant)(Fig.1). This feature is very different from TL curve from ordinary calcite (Fig. 2), but similar to that of aragonite. Most of the emission around 360℃ is not due to radiation damage accumulated in the natural environment, but rather due to filling traps through the mineral growth from the start. To find out the reason for this calcite having a different trap nature from ordinal calcite, examination of crystallinity estimated from XRD data, trace element concentration from LAICPMS data, and effect by sample preparation methods, was carried out, but no clear interpretation was possible. Based on the geological observation where samples were collected, the calcite analyzed here could contaminated with more organic carbon (although, measured samples did not contain much of H_2O_2 solubles) than other ordinal calcite. The unusual emission might be caused from this contamination.
To extract TL originated from the radiation induced traps, peak separation was performed to eliminate the influence of the peak from the high temperature side which is the light emission derived from the original trap fill. Accumulated dose was calculated by using the signal of 200 to 280 ° C derived from radiation damage by the Multi aliquot additive dose method (Aitken, 1985). As a result, all the measured sample show dates much older than 100,000 years. However, these samples are precipitated from current alkaline water flow, and are expected to be in a relatively young age (around 2000 to 10000 years), suggested by the 14C age of carbonate and organic matter collected in the area. It is considered that part of traps responsible for peaks existing at 200 to 280℃ was also filled originally, but not by radiation. In order to measure the accumulated dose more accurately, further research on identification of the precise peak position of this sample and emission existed just after the crystal precipitation is necessary.

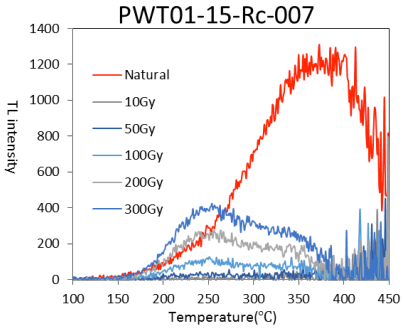

Fig. 1. Example of natural (red line) and artificial (others) TL glow curve.

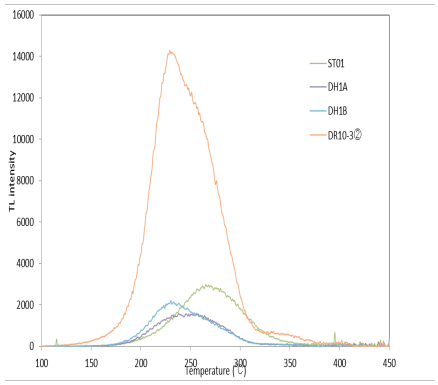

Fig. 2. Example of natural TL glow curve from ordinary calcite.

CO5-18 Studies on the Binding Mechanism and Stoichiometry of Mercury Atoms in an Organomercury Lyase from Smeared Solution by an *in-cell* Radioactivation Analysis

K. Takamiya and Y. Morimoto

Institute for Integrated Radiation and Nuclear Science, Kyoto University

INTRODUCTION: The organomercury lyase (MerB) catalyzes the protonolysis of the carbon-mercury bonding and produces an ionic mercury and hydrocarbon. The ionic mercury [Hg(II)] is immediately reduced to less reactive mercury [Hg(0)] by a mercuric reductase (MerA). The MerB enzyme has three active amino acids in an active site, and they hold stoichiometrically one Hg atom by Cys-SH or Asp-COOH / Hg-C bonding. We have determined the tertiary structure of the enzyme at atomic resolution, and considered a pathway of Hg compound via solution. And other research point, structure based mercury capture system will be proposed to decrease toxic mercury in the environment. It is available for non-energetic mercury detox by use of bacterial bio-remediation. In the evaluation of mercury recover from solution or cultivation medium, radioactivation analysis is available rather than an ICP-mass spectroscopy in particular intact cell analysis. We have checked and pre-evaluated mercury content in a standard mercury solution by a measurement of γ-ray after irradiation of neutron in the KUR.

EXPERIMENTS: Cultivation of over-expression system of the *E.coli* (BL21-DE3) and sampling procedures are shown in the figure 1.

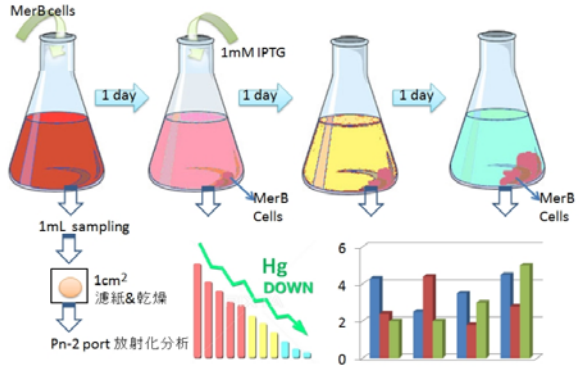

Fig.1 A schematic drawing of cultivation of the *E.coli* harboring MerB and medium sampling to radioactivation analysis

In a cultivation of the *E.coli*, minimum medium based on the ILL deuterium lab was used to keep surplus reagents away from bacterium growth. Several millimolar mercury reagent (Hg_2I_2, CH_3HgI, C_2H_5HgCl, CH_3HgCl, $HgNO_3/H_2O$, $HgCl_2$, HgCl and $Hg(CH_3COO)_2$) solutions are prepared and used. Neutron irradiation was curried out at Pn-2 port at the KUR operated by 5MW.

RESULTS and DISCUSSION: In the enzyme structure an Hg atom is found at active site[1)] in the CH_3HgCl additive preparation and is stoichiometrically held as one Hg-atom (Fig.2), a dimer enzyme has two Hg atoms. And also there is no CH_3HgCl compound, it suggests that Hg atom is isolated by bond-braking between Hg-C.

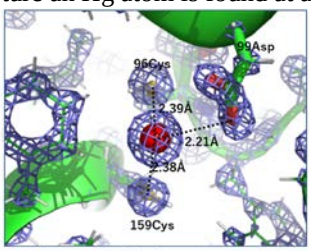

Fig.2 An Hg atom held by three amino acids. Electron densities are presented by cage.

The enzyme prepared by the previous minimum medium cultivation and purification has enough activity to donate proton into the Hg compound and protonolysis Hg-C bonding.

In a radioactivation analysis by neutron irradiation, it is essential how limit of under concentration of Hg atoms in the enzyme or solution. Since in the structural analysis the CH_3HgCl is suitable for enzymatic activity and structural stability, its solution is used as standard solution with three kinds of concentration of 5mM, 0.5mM and 0.05mM. Filter papers (1 x 1 cm) soaked by 500μL of each solution are used for evaluation of γ-ray. A decay of the Hg is led by the following process (Fig.3).

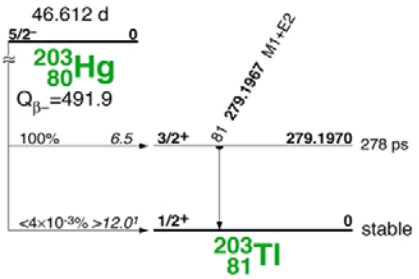

Fig.3 A typical scheme of ^{203}Hg decay in a $^{202}Hg(n,\gamma)$ reaction.

The γ-ray spectrometry was carried out by the Canberra GC 4020 Ge- detector within two weeks. Neutron exposure time was 60 seconds at 5MW reactor operation.

A high concentration (5mM) sample out of three solutions gives an efficient γ-ray within error of 1%, but other two concentrations have large errors under the same condition in the case of 5mM solution. We have obtained information of the irradiation time over 60 seconds for 0.5 and 0.05mM concentration solutions and precise evaluation of the mercury content is now still going.

REFFERENCE:

1) A study of preparation and structural analysis of the organomercury lyase for a neutron diffraction experiment. Y.Morimoto and A.Kita, Annual meeting of the KURRI 2017